

Interpretation of $Y_b(10750)$ as a tetraquark and its production mechanism

Ahmed Ali*

Deutsches Elektronen-Synchrotron DESY, D-22607 Hamburg, Germany

Luciano Maiani†

*T. D. Lee Institute, Shanghai Jiao Tong University, Shanghai, 200240, China and
Dipartimento di Fisica and INFN, Sapienza Università di Roma, Piazzale Aldo Moro 2, I-00185 Roma, Italy*

Alexander Ya. Parkhomenko‡

Department of Theoretical Physics, P. G. Demidov Yaroslavl State University, Sovietskaya 14, 150003 Yaroslavl, Russia

Wei Wang§

*INPAC, SKLPPC, MOE KLPPC, School of Physics and Astronomy,
Shanghai Jiao Tong University, Shanghai 200240, China*

(Dated: August 23, 2021)

Recently, the Belle Collaboration has updated the analysis of the cross sections for the processes $e^+e^- \rightarrow \Upsilon(nS)\pi^+\pi^-$ ($n = 1, 2, 3$) in the e^+e^- center-of-mass energy range from 10.52 to 11.02 GeV. A new structure, called here $Y_b(10750)$, with the mass $M(Y_b) = (10752.7 \pm 5.9_{-1.1}^{+0.7})$ MeV and the Breit-Wigner width $\Gamma(Y_b) = (35.5_{-11.3-3.3}^{+17.6+3.9})$ MeV was observed [1]. We interpret $Y_b(10750)$ as a compact $J^{PC} = 1^{--}$ state with a dominant tetraquark component. The mass eigenstate $Y_b(10750)$ is treated as a linear combination of the diquark-antidiquark and $b\bar{b}$ components due to the mixing via gluonic exchanges shown recently to arise in the limit of large number of quark colors. The mixing angle between Y_b and $\Upsilon(5S)$ can be estimated from the electronic width, recently determined to be $\Gamma_{ee}(Y_b) = (13.7 \pm 1.8)$ eV. The mixing provides a plausible mechanism for $Y_b(10750)$ production in high energy collisions from its $b\bar{b}$ component and we work out the Drell-Yan and prompt production cross sections for $pp \rightarrow Y_b(10750) \rightarrow \Upsilon(nS)\pi^+\pi^-$ at the LHC. The resonant part of the dipion invariant mass spectrum in $Y_b(10750) \rightarrow \Upsilon(1S)\pi^+\pi^-$ and the corresponding angular distribution of π^+ -meson in the dipion rest frame are presented as an example.

1. Introduction

Recently, Belle has reported an updated measurement of the cross sections for $e^+e^- \rightarrow \Upsilon(nS)\pi^+\pi^-$; $nS = 1S, 2S, 3S$ in the e^+e^- center-of-mass energy range from 10.52 to 11.02 GeV. They observe a new structure, $Y_b(10750)$, in addition to the $\Upsilon(10860)$ - and $\Upsilon(11020)$ -resonances, having the masses and Breit-Wigner decay widths shown in Table I [1]. The measured ranges of the product $\Gamma_{ee} \times \mathcal{B}$ (in eV) for the three final states are also presented in Table I. The global significance of the new structure is 5.2σ . We recall that in high statistics energy scans for the ratios $R_{\Upsilon\pi^+\pi^-} \equiv \sigma(e^+e^- \rightarrow (\Upsilon(1S), \Upsilon(2S), \Upsilon(3S))\pi^+\pi^-) / \sigma(e^+e^- \rightarrow \mu^+\mu^-)$ and $R_{b\bar{b}} \equiv \sigma(e^+e^- \rightarrow b\bar{b}) / \sigma(e^+e^- \rightarrow \mu^+\mu^-)$, Belle had found no new structures in their 2016 analysis [2]. In the same analysis, a 90% C.L. upper limit of 9 eV was set on Γ_{ee} in search of a structure around 10.9 GeV in $R_{b\bar{b}}$ [2]. We also recall that the visible cross section for $e^+e^- \rightarrow B_s^{(*)}\bar{B}_s^{(*)}$ showed a clear peak for $\Upsilon(10860)$, a less clear one for the $\Upsilon(11020)$, but no significant signal was observed around 10.75 GeV [3].

The combined BaBar and Belle data on $R_{b\bar{b}}$ have been recently reanalyzed taking into account the coherent sum of the three resonances $\Upsilon(10860)$, $\Upsilon(11020)$, and $Y_b(10750)$ [4], and a continuum amplitude, proportional to $1/\sqrt{s}$, where \sqrt{s} is the center-of-mass e^+e^- energy. The fit parameters of the $R_{b\bar{b}}$ lineshape are the masses, Breit-Wigner decay widths, leptonic partial decay widths, and the relative phases. The resulting resonance masses and decay widths are found to be in agreement with the ones obtained from the $R_{\Upsilon\pi^+\pi^-}$ scan, and one gets a number of solutions for the partial electronic widths (mathematically 8 solutions are expected), which differ in other parameters, such as the total decay widths and partial leptonic widths. Most of these solutions are likely unphysical except the first solution, in which the electronic width of Y_b is given as [4]:

$$\Gamma_{ee}(Y_b(10750)) = (13.7 \pm 1.8) \text{ eV.} \quad (1)$$

In this paper, we interpret $Y_b(10750)$ as a $J^{PC} = 1^{--}$ tetraquark candidate, whose dominant component Y_b^0 consists of a colored diquark-antidiquark pair $[bq]_{\bar{3}_c}[\bar{b}\bar{q}]_{3_c}$, bound in the $SU(3)$ antitriplet-triplet representation [5, 6]. However, it can have a small $b\bar{b}$ component due to the mixing via gluonic exchanges. The behavior of QCD for large- N_c , where N_c is the number of colors, has been worked out long ago by 't Hooft [7]. With the quark-gluon coupling as $L_{\text{QCD}} = g_{\text{QCD}}\bar{q}\lambda^A g_\mu^A \gamma^\mu q$ and λ^A being the $N_c^2 - 1$ $SU(N_c)$ matrices, the large- N_c limit is consid-

* Corresponding Author, Email: ahmed.ali@desy.de

† Corresponding Author, Email: luciano.maiani@cern.ch

‡ Corresponding Author, Email: parkh@uniyar.ac.ru

§ Corresponding Author, Email: wei.wang@sjtu.edu.cn

TABLE I. Measured masses and decay widths (in MeV), and ranges of $\Gamma_{ee} \times \mathcal{B}$ (in eV) of the $\Upsilon(10860)$, $\Upsilon(11020)$, and the new structure $Y_b(10750)$. The first uncertainty is statistical and the second is systematic (Belle [1]).

State	$\Upsilon(10860)$	$\Upsilon(11020)$	$Y_b(10750)$
Mass	$10885.3 \pm 1.5^{+2.2}_{-0.9}$	$11000.0^{+4.0+1.0}_{-4.5-1.3}$	$10752.7 \pm 5.9^{+0.7}_{-1.1}$
Width	$36.6^{+4.5+0.5}_{-3.9-1.1}$	$23.8^{+8.0+0.7}_{-6.8-1.8}$	$35.5^{+17.6+3.9}_{-11.3-3.3}$
$\Upsilon(1S)\pi^+\pi^-$	0.75 – 1.43	0.38 – 0.54	0.12 – 0.47
$\Upsilon(2S)\pi^+\pi^-$	1.35 – 3.80	0.13 – 1.16	0.53 – 1.22
$\Upsilon(3S)\pi^+\pi^-$	0.43 – 1.03	0.17 – 0.49	0.21 – 0.26

ered as $g_{\text{QCD}} \rightarrow 0$, $g_{\text{QCD}}^2 N_c \equiv \lambda$ fixed. The amplitudes are expanded in powers of $1/N_c$, with each term being a nonperturbative function of the reduced coupling λ . As explained below (see Fig. 1), it implies that $\Upsilon(10860)$ and $\Upsilon(11020)$, which are dominantly radial $b\bar{b}$ excitations, $\Upsilon(5S)$ and $\Upsilon(6S)$, respectively, also have a small diquark-antidiquark component Y_b^0 in their Fock space. Due to the proximity of the mass eigenstates $Y_b(10750)$ and $\Upsilon(10860)$, we consider that the mixing is dominantly between Y_b^0 and $\Upsilon(5S)$. This also provides a plausible interpretation of some anomalous features measured in the decays of the $\Upsilon(10860)$.¹

We argue that the production mechanism of $Y_b(10750)$ proceeds through its $b\bar{b}$ component, which arises from the mixing $([bq]_{3_c}[\bar{b}\bar{q}]_{3_c} - b\bar{b})$. A non-vanishing mixing is induced by non-planar diagrams [12], allowing the direct production of $Y_b(10750)$ in high energy collisions. Using this, Drell-Yan [13] and prompt production cross sections [14] for $Y_b(10750)$ are presented for the LHC. We estimate the $Y_b - \Upsilon(5S)$ mixing angle from $\Gamma_{ee}(Y_b)$ in Eq. (1)

In contrast to the decays of $\Upsilon(10860)$ and $\Upsilon(11020)$, whose dipionic transitions ($\Upsilon(1S)$, $\Upsilon(2S)$, $\Upsilon(3S)$) $\pi^+\pi^-$ are dominated by the resonant $Z_b^\pm(10650)$ and $Z_b^\pm(10610)$ states [15], the decay $Y_b(10750) \rightarrow Z_b^\pm(10650)\pi^\mp$ is kinematically forbidden, and $Y_b(10750) \rightarrow Z_b^\pm(10610)\pi^\mp$ has a strong phase-space suppression. Thus, $Y_b(10750)$ decays are anticipated to reflect their dominant non-resonant component. In addition, the decays $Y_b \rightarrow (\Upsilon(1S), \Upsilon(2S), \Upsilon(3S))\pi^+\pi^-$, being Zweig-allowed, are anticipated to have decay widths characteristic of strong interactions. Dalitz analysis in the decay $Y_b \rightarrow \Upsilon(1S)\pi^+\pi^-$ will show a

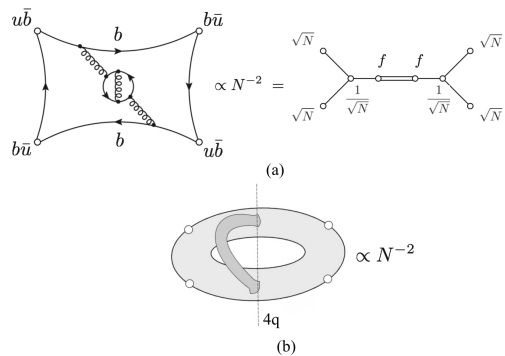


FIG. 1. (a) Left-hand side: lowest order diagram for meson-meson scattering that may have quarkonium and four-quark poles connected by mixing, as indicated by the diagram on the right-hand side, see Eq. (2). (b) Topological structure of the nonperturbative realization of the same process. N denotes the number of colors.

band structure in the $m_{\pi^+\pi^-}$ invariant mass, revealing clear evidence of two scalars, $f_0(500)$ and $f_0(980)$, and the tensor $J^{PC} = 2^{++}$ meson, $f_2(1270)$ [16]. In other two decays $Y_b \rightarrow (\Upsilon(2S), \Upsilon(3S))\pi^+\pi^-$, only the broad $f_0(500)$ -meson is present. With higher statistics data anticipated with the Belle-II detector, this distribution, as well as other properties of $Y_b(10750)$, will be well measured, allowing us to discriminate the tetraquark picture from other competing mechanisms, such as a D -wave interpretation of $Y_b(10750)$, with a large $S - D$ mixing [17].

2. Tetraquark- $Q\bar{Q}$ mixing in large- N_c approach

In a seminal paper, S. Weinberg [18] addressed the description of tetraquarks in the large- N_c limit, followed by several investigations [12, 19–24]. A mixing between a bottomonium and hidden-beauty tetraquark, anticipated in [19], was shown in [12], to be induced at the level of non-planar diagrams, Fig. 1(a) and (b).

In brief, the exchange of a gluon between the two quark loops in Fig. 1(a) produces the interaction by which a genuine tetraquark pole may form in the intermediate state. Fig. 1(b) displays the non-perturbative version of Fig. 1(a). In the language introduced by 't Hooft for the large- N_c expansion [7], non-planar gluon exchanges between the two fermion loops mean topologically one handle and produce a mixing coefficient f of order²

$$f = \frac{1}{N_c \sqrt{N_c}}. \quad (2)$$

¹ A tetraquark interpretation [8, 9] had been put forward for the $Y_b(10890)$, a resonance observed by Belle more than a decade ago [10, 11], together with $Y_b(10860)$, identified with $\Upsilon(5S)$. In subsequent data by Belle [2], two states $Y_b(10890)$ and $\Upsilon(10860)$ were found to have the same mass within 2σ , essentially closing the window for an additional resonance. This seems to have changed with the announcement of $Y_b(10750)$.

² In the large- N_c language, an amplitude \mathcal{A} for a process has the dependence $\mathcal{A} \propto N_c^\alpha$, where $\alpha = 2 - L - 2H$, with L being the number of fermion loops and H the number of handles, i. e. independent non-planar sets of gluons. For a planar diagram $H = 0$ and $L = 1$, yielding $\alpha = 1$. Large- N_c -counting rules in the context of tetraquarks are given in [25].

A non-vanishing mixing with charmonia is also predicted in the alternative extension to large N_c based on Witten's picture of large- N_c baryons [26]. These "generalized tetraquarks" are made by $N_c - 1$ antisymmetric quarks bound to $N_c - 1$ antisymmetric antiquarks [27–30]. Non-vanishing mixing with quarkonia has been noted in [31]. Albeit suppressed at large N_c by the exponential factor $e^{-N_c/2}$, when extrapolated back to $N_c = 3$ one finds a result not dissimilar from (2). Thus, production in the e^+e^- -annihilation of resonances such as $Y_b(10750)$, in addition to the bottomonia spectral lines and with a small Γ_{ee} , is a significant signature of tetraquarks.

3. Mixing formalism

Following [8, 9], we define the tetraquark states Y_b^I in the isospin basis, with the $Y_b^0 \equiv (Y_{[bu]} + Y_{[bd]})/\sqrt{2}$ and $Y_b^1 \equiv (Y_{[bu]} - Y_{[bd]})/\sqrt{2}$ for isospin $I = 0$ and $I = 1$, respectively. We ignore their mass difference due to the isospin breaking. Since the production is via the isosinglet $b\bar{b}$ -component, we consider only Y_b^0 , the isospin-0 state. In view of the observed mass difference (see Table I) $M[\Upsilon(10860)] - M[Y_b(10750)] \simeq 133$ MeV, compared to the mass difference $M[\Upsilon(11020)] - M[Y_b(10750)] \simeq 247$ MeV, we only consider the mixing between $\Upsilon(10860)$ and $Y_b(10750)$, though it can be generalized to the case with all three states.

Mass eigenstates are rotated from the eigenstates in the quark flavor space, with the latter defined as $\Upsilon(5S)$ and Y_b^0 , respectively.

$$\begin{pmatrix} Y_b(10750) \\ \Upsilon(10860) \end{pmatrix} = \begin{pmatrix} \cos \tilde{\theta} & \sin \tilde{\theta} \\ -\sin \tilde{\theta} & \cos \tilde{\theta} \end{pmatrix} \begin{pmatrix} Y_b^0 \\ \Upsilon(5S) \end{pmatrix}, \quad (3)$$

where $\tilde{\theta}$ is a mixing angle, estimated below phenomenologically. This mixing relates $\Gamma_{ee}[Y_b(10750)]$ and $\Gamma_{ee}[\Upsilon(5S)]$, yielding

$$\frac{\Gamma_{ee}[Y_b(10750)]}{\Gamma_{ee}[\Upsilon(10860)]} = \tan^2 \tilde{\theta} \left[\frac{M[\Upsilon(10860)]}{M[Y_b(10750)]} \right]^4 \simeq 1.04 \tan^2 \tilde{\theta}. \quad (4)$$

Recalling that $\Gamma_{ee}[\Upsilon(10860)] = (310 \pm 70)$ eV [16], and the recent value given in (1), we find

$$\tan^2 \tilde{\theta} = 0.044 \pm 0.006, \quad (5)$$

which leads to $\tilde{\theta} \sim 12^\circ$.

4. Hadroproduction and Drell-Yan cross sections for $pp \rightarrow Y_b(10750) \rightarrow \Upsilon(nS) \pi^+ \pi^-$ at the LHC

In Ref. [14], the hadroproduction cross sections for $\Upsilon(5S)$ and $\Upsilon(6S)$ in $p\bar{p}$ and pp collisions were calculated at the Tevatron and LHC, using the Non-Relativistic QCD framework [32]. The calculation has adopted a factorization ansatz to separate the short- and long-distance effects.

First, cross-sections for $Y_b(10750)$ are scaled from the ones for $\Upsilon(5S)$, since the production takes place via the $b\bar{b}$ -component in the $Y_b(10750)$ Fock space. The latter is determined by the mixing angle, derived in the previous section, and results in the following relation:

$$\begin{aligned} & \frac{\sigma(pp \rightarrow Y_b(10750) + X) \mathcal{B}_f(Y_b)}{\sigma(pp \rightarrow \Upsilon(10860) + X) \mathcal{B}_f(\Upsilon(10860))} \\ & \simeq \frac{\Gamma_{ee}(Y_b) \mathcal{B}_f(Y_b)}{\Gamma_{ee}(\Upsilon(10860)) \mathcal{B}_f(\Upsilon(10860))}. \end{aligned} \quad (6)$$

Here, $\mathcal{B}_f(Y_b)$ and $\mathcal{B}_f(\Upsilon(10860))$ denote the branching ratios of $Y_b(10750) \rightarrow f$ and $\Upsilon(10860) \rightarrow f$, respectively, where f represents the three dipionic final states $\Upsilon(1S)\pi^+\pi^-$, $\Upsilon(2S)\pi^+\pi^-$, and $\Upsilon(3S)\pi^+\pi^-$. The r.h.s. of Eq. (6) has been measured by Belle [1].

Secondly, to obtain the absolute cross section for $Y_b(10750)$ production, we estimate the $\Upsilon(10860)$ cross section in NRQCD, following the calculation presented in [14]. One starts from the formula:

$$\begin{aligned} \sigma(pp \rightarrow \Upsilon(10860) + X) &= \sum_Q \sigma_Q \\ &= \sum_Q \int dx_1 dx_2 \sum_{i,j} f_i(x_1) f_j(x_2) \\ &\quad \times \hat{\sigma}(ij \rightarrow \langle b\bar{b} \rangle_Q + X) \langle O[Q] \rangle. \end{aligned} \quad (7)$$

Here, i and j denote a generic parton inside a proton, $f_i(x_1)$ and $f_j(x_2)$ are the parton distribution functions (PDFs) [33], the label Q denotes the quantum numbers of the $b\bar{b}$ -pair, which are labeled as ${}^{2S+1}L_J^c$ (color c , spin S , orbital angular momentum L and total angular momentum J), $\langle O[Q] \rangle$ are the corresponding long-distance matrix elements (LDMEs), and $\hat{\sigma}$ is a partonic cross section.

The leading-order partonic processes for the S -wave configurations are:

$$\begin{aligned} g + g &\rightarrow \Upsilon[{}^3S_1^1] + g, \\ g + g &\rightarrow \Upsilon[{}^1S_0^8, {}^3S_1^8] + g, \\ g + q &\rightarrow \Upsilon[{}^1S_0^8, {}^3S_1^8] + q, \\ q + \bar{q} &\rightarrow \Upsilon[{}^1S_0^8, {}^3S_1^8] + g. \end{aligned} \quad (8)$$

The normalized cross sections, in which the LDMEs are factored out, are defined by $\tilde{\sigma}_Q \equiv \sigma_Q / \langle O[Q] \rangle$. They have been calculated in Ref. [14] for the LHC energies $\sqrt{s} = 7, 8$ and 14 TeV. They are supplemented by the LDMEs, for which the following values have been used. The LDME of the Color-Singlet ${}^3S_1^1$ is $\langle O[Q] \rangle \simeq 0.56$ GeV³; the Color-Octet LDMEs, for ${}^1S_0^8$ and ${}^3S_1^8$, are estimated as $\langle O[Q] \rangle = (-0.95 \pm 0.38) \times 10^{-3}$ GeV³, and $\langle O[Q] \rangle = (3.46 \pm 0.21) \times 10^{-2}$ GeV³, respectively. Summing over the partonic processes shown above, and using the branching ratios from the PDG, yields the cross sections $\sigma(pp \rightarrow \Upsilon(5S) \rightarrow (\Upsilon(nS) \rightarrow \mu^+ \mu^-) \pi^+ \pi^-)$, where $n = 1, 2, 3$ [14].

The corresponding cross sections for the processes $pp \rightarrow Y_b(10750) \rightarrow (\Upsilon(nS) \rightarrow \mu^+ \mu^-) \pi^+ \pi^-$ are obtained by using the scaling relation given in Eq. (6). For

TABLE II. Total cross sections (in pb) for the processes $pp \rightarrow Y_b(10750) \rightarrow (\Upsilon(nS) \rightarrow \mu^+\mu^-)\pi^+\pi^-$ ($n = 1, 2, 3$) at the LHC ($\sqrt{s} = 14$ TeV), assuming the transverse momentum range $3 \text{ GeV} < p_T < 50 \text{ GeV}$. The rapidity range $|y| < 2.5$ is used for ATLAS and CMS (called LHC 14), and the rapidity range $2.0 < y < 4.5$ is used for the LHCb. The error estimates in the QCD production are from the variation of the central values of the Color-Octet LDMEs and the various decay branching ratios, as discussed in Ref. [14]. Contributions from $\Upsilon(1S, 2S, 3S)$ are added together in the Drell-Yan production mechanism as in Ref. [13].

	QCD (gg)			Drell-Yan
	$n = 1$	$n = 2$	$n = 3$	DY
LHC 14	[0.29, 3.85]	[0.70, 4.78]	[0.45, 3.10]	[0.002, 0.004]
LHCb 14	[0.08, 1.21]	[0.20, 1.51]	[0.13, 0.99]	[0.001, 0.002]

the LHC at $\sqrt{s} = 14$ TeV, cross sections are given in Table II for the indicated ranges of $p_T(Y_b)$ and rapidity $|y|$, separately for ATLAS/CMS and for LHCb. Theoretical uncertainties in these cross sections are almost a factor 10, dominated by the uncertainties on the Color-Octet LDMEs, as well as on the ratio on the r.h.s. in Eq. (6). To estimate the expected number of events, we use 1 pb for the cross section, which lies in the middle of the indicated ranges, yielding $O(10^4)$ signal events at the LHCb, and an order of magnitude larger for the other two experiments, ATLAS and CMS. The discovery channel $\mu^+\mu^-\pi^+\pi^-$, with the $\mu^+\mu^-$ mass constrained by the $\Upsilon(nS)$ ($nS = 1S, 2S, 3S$) masses, involves a pair of charged pions. Thus, the background is a stumbling block, but hopefully this can be overcome, with the additional constraint of the $Y_b(10750)$ mass. In addition to the mixing mechanism utilized here, there maybe direct production of the tetraquark, which would add incoherently to the previous results. Thus, the numbers presented in Table II give lower bounds to the expected $Y_b(10750)$ production in pp collisions.

The Drell-Yan production cross sections and differential distributions in the transverse momentum and rapidity of the $J^{PC} = 1^{--}$ exotic hadrons $\phi(2170)$, $X(4260)$ and $Y_b(10890)$ at the hadron colliders LHC and Tevatron have been calculated in [13]. We update these calculations for the production of $Y_b(10750)$ at the LHC for $\sqrt{s} = 14$ TeV, and present results for $pp \rightarrow Y_b(10750) \rightarrow (\Upsilon(nS) \rightarrow \mu^+\mu^-)\pi^+\pi^-$ taking into account the current mass of $Y_b(10750)$ and the measured quantity $\Gamma_{ee} \times \mathcal{B}$, whose ranges are measured by Belle [1] and given in Table I. In deriving the distributions and cross sections, we have included the order α_s QCD corrections, resummed the large logarithms in the small transverse momentum region in the impact-parameter formalism, and have used two sets of parton distribution functions: MSTW (Martin-Stirling-Thorne-Watt) PDFs [34] and CTEQ10 [35]; the details can be seen in [13]. Numerical results for the cross section are given in Table II, where the p_T and rapidity $|y|$ ranges for the ATLAS and CMS (called LHC 14 there), and for the LHCb, are indicated. These cross sections yield $O(300)$ events for the current ATLAS/CMS luminosity (140 fb^{-1}), and $O(10)$ events for the LHCb (9 fb^{-1}), but could be higher by a factor 2. The Drell-Yan cross sections are theoretically

more accurate, but suffer from the small rates compared to the hadroproduction cross sections at the LHC.

5. Dipion invariant mass spectra and angular distributions in $e^+e^- \rightarrow Y_b \rightarrow \Upsilon(nS)\pi^+\pi^-$

The amplitudes of the $e^+e^- \rightarrow Y_b \rightarrow \Upsilon(nS)PP'$ process, where $P^{(\prime)}$ is a pseudoscalar, have been calculated in [9] as a sum of the Breit-Wigner resonances and non-resonating continuum contributions, with the latter adopted from [36]. The differential cross section is then written as [9]:

$$\frac{d^2\sigma_{\Upsilon(1S)PP'}}{dm_{PP'} d\cos\theta} = \frac{\lambda^{1/2}(s, m_\Upsilon^2, m_{PP'}^2)\lambda^{1/2}(m_{PP'}^2, m_P^2, m_{P'}^2)}{384\pi^3 s m_{PP'} [(s - m_{Y_b}^2)^2 + m_{Y_b}^2 \Gamma_{Y_b}^2]} \times \left\{ \left(1 + \frac{(q \cdot p)^2}{2s m_\Upsilon^2} \right) |\mathcal{S}|^2 + 2 \text{Re} \left[\mathcal{S}^* \left(\mathcal{D}' + \frac{(q \cdot p)^2}{2s m_\Upsilon^2} \mathcal{D}'' \right) \right] \left(\cos^2\theta - \frac{1}{3} \right) + |\mathcal{D}|^2 \sin^2\theta \left[\sin^2\theta + 2 \left(\frac{q_0^2}{s} + \frac{p_0^2}{m_\Upsilon^2} \right) \cos^2\theta \right] + \left(|\mathcal{D}'|^2 + \frac{(q \cdot p)^2}{2s m_\Upsilon^2} |\mathcal{D}''|^2 \right) \left(\cos^2\theta - \frac{1}{3} \right)^2 \right\}, \quad (9)$$

where s and $m_{PP'}$ are the squared invariant masses of the e^+e^- -pair and a pair of two final pseudoscalars, θ is the angle between the momenta of Y_b and P in the PP' rest frame, $\lambda(x, y, z) \equiv (x - y - z)^2 - 4yz$, q_0 and p_0 are the energies of the Y_b - and $\Upsilon(1S)$ -mesons in the PP' rest frame, respectively, Γ_{Y_b} is the decay width of Y_b , and m_{Y_b} , m_Υ , m_P and $m_{P'}$ are the masses of Y_b , $\Upsilon(1S)$, P and P' , respectively.

The S -wave amplitude for the PP' system, \mathcal{S} , and the D -wave amplitudes, \mathcal{D} , \mathcal{D}' and \mathcal{D}'' , are the sums over possible isospin states:

$$\mathcal{M} = \sum_I \mathcal{M}_I \quad \text{for } \mathcal{M} = \mathcal{S}, \mathcal{D}, \mathcal{D}', \mathcal{D}'', \quad (10)$$

where $I = 0$ for $\pi^+\pi^-$, $I = 0, 1$ for K^+K^- , and $I = 1$ for $\eta\pi^0$. Details are given in [9].

We concentrate on the process $Y_b(10750) \rightarrow \Upsilon(1S)\pi^+\pi^-$, in which the $\sigma = f_0(500)$, $f_0(980)$, and

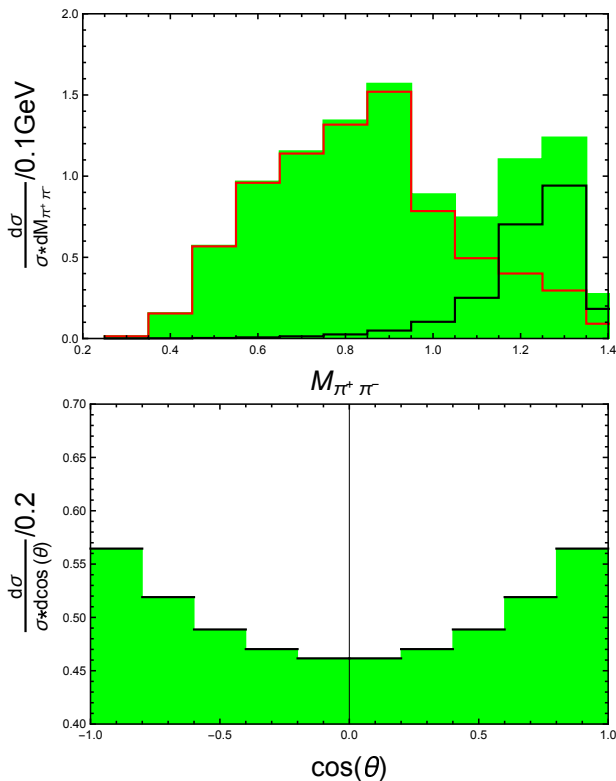


FIG. 2. The normalized resonant $m_{\pi^+\pi^-}$ (upper plot) and $\cos\theta$ (lower plot) distributions for $e^+e^- \rightarrow Y_b(10750) \rightarrow \Upsilon(1S)\pi^+\pi^-$ are shown using the coupling constants obtained in [9] (green histogram). The contributions from $f_0(500)$ and $f_0(980)$ scalars (left red curve) and $f_2(1270)$ (right black curve) are indicated in the upper plot.

$f_2(1270)$ resonances contribute. The $I = 0$ amplitudes are given by the combinations of the resonance amplitudes, \mathcal{M}_0^S and $\mathcal{M}_0^{f_2}$, and the non-resonating continuum amplitudes, \mathcal{M}_0^{1C} and \mathcal{M}_0^{2C} :

$$\begin{aligned} \mathcal{S}_0 &= \mathcal{M}_0^{1C} + (k_1 \cdot k_2) \sum_S \mathcal{M}_0^S, & \mathcal{D}_0 &= |k|^2 \mathcal{M}_0^{f_2}, \\ \mathcal{D}'_0 &= \mathcal{M}_0^{2C} - \mathcal{D}_0, & \mathcal{D}''_0 &= \mathcal{M}_0^{2C} + \frac{2q_0 p_0}{(q \cdot p)} \mathcal{D}_0, \end{aligned} \quad (11)$$

where S runs over possible $I = 0$ scalar resonances, and $|k|$ is the magnitude of the π^+ -meson three momentum in the $\pi^+\pi^-$ rest frame. The $m_{\pi^+\pi^-}$ and $\cos\theta$ distributions for $e^+e^- \rightarrow Y_b \rightarrow \Upsilon(1S)\pi^+\pi^-$, normalized by the measured cross section $\sigma_{\Upsilon(1S)\pi^+\pi^-}^{\text{Belle}} = (1.61 \pm 0.16)$ pb of the older Belle data [10] were fitted in [9], which determined various coupling constants. Since these distributions are not available for the new Belle data [1], we show in Fig. 2 only the resonant contributions, using the relevant in-

put parameters from [9]. This illustrates the anticipated spectral shapes, which will be modified in detail as the non-resonant contribution is included. The fit can only be undertaken as the experimental measurements become available.

The products $\Gamma_{ee} \times \mathcal{B}$ are measured by Belle, and we take $\Gamma_{ee}[Y_b(10750)]$ from (1). The corresponding ranges are (0.9 – 3.4)% for $\mathcal{B}_{\Upsilon(1S)\pi^+\pi^-}$, (3.9 – 8.9)% for $\mathcal{B}_{\Upsilon(2S)\pi^+\pi^-}$, and (1.5 – 1.9)% for $\mathcal{B}_{\Upsilon(3S)\pi^+\pi^-}$. They are in a reasonable range for the Zweig-allowed decays. We also note that due to the dominant tetraquark nature of $Y_b(10750)$, and its quark content, decays $Y_b(10750) \rightarrow B_s^{(*)} \bar{B}_s^{(*)}$ are not anticipated, in agreement with the Belle data [3].

6. Summary

In this work, we have presented a tetraquark-based interpretation of the Belle data on the new structure $Y_b(10750)$ in e^+e^- annihilation, invoking the tetraquark- $b\bar{b}$ mixing anticipated in the large- N_c limit. The $b\bar{b}$ -component is used to predict the hadroproduction and Drell-Yan cross sections at the LHC. A crucial test of our model is in the $m_{\pi^+\pi^-}$ and $\cos\theta$ distributions, whose resonant contribution is worked out, which is not expected in other dynamical schemes, such as $Y_b(10750)$ interpreted as a D -wave $b\bar{b}$ state, with a very large $S - D$ mixing [17]. The tetraquark- $Q\bar{Q}$ mixing scheme suggested here has wider implications.

Acknowledgements

We thank Changzheng Yuan for informing us of his preliminary results on the electronic width of $Y_b(10750)$ and Satoshi Mishima for his help in checking our code for the distributions shown in Fig. 2 and helpful correspondence. The present work was stimulated by discussions at the Workshop on Exotic Hadrons held at the T.D. Lee Institute, Shanghai, June 25–27, 2019, and INPAC, Shanghai Key Laboratory for Particle Physics and Cosmology. The work of W. W. is supported in part the National Natural Science Foundation of China under Grant Nos. 11575110, 11735010, 11911530088, and the Natural Science Foundation of Shanghai under Grant No. 15DZ2272100. A.P. and W.W. acknowledge financial support by the Russian Foundation for Basic Research and National Natural Science Foundation of China according to the joint research project (Nos. 19-52-53041 and 1181101282). This research is partially supported by the “YSU Initiative Scientific Research Activity” (Project No. AAAA-A16-116070610023-3).

[1] R. Mizuk *et al.* [Belle Collaboration], JHEP **1910**, 220 (2019) [arXiv:1905.05521v4[hep-ex]].

[2] D. Santel *et al.* [Belle Collaboration], Phys. Rev. D **93**, 011101 (2016) [arXiv:1501.01137 [hep-ex]].

- [3] A. Abdesselam *et al.*, arXiv:1609.08749 [hep-ex].
- [4] Chang-Zheng Yuan in *XVth Rencontres du Vietnam*, September 22nd – 28th, 2019, Quy Nhon, Vietnam. Mathematically, more solutions for $\Gamma_{ee}(Y_b)$ are allowed.
- [5] R. L. Jaffe and F. Wilczek, Phys. Rev. Lett. **91**, 232003 (2003) [hep-ph/0307341].
- [6] L. Maiani, F. Piccinini, A. D. Polosa and V. Riquer, Phys. Rev. D **71**, 014028 (2005) [hep-ph/0412098].
- [7] G. 't Hooft, Nucl. Phys. B **72**, 461 (1974).
- [8] A. Ali, C. Hambroek and M. J. Aslam, Phys. Rev. Lett. **104**, 162001 (2010) Erratum: [Phys. Rev. Lett. **107**, 049903 (2011)] [arXiv:0912.5016 [hep-ph]].
- [9] A. Ali, C. Hambroek and S. Mishima, Phys. Rev. Lett. **106**, 092002 (2011) [arXiv:1011.4856 [hep-ph]].
- [10] K. F. Chen *et al.* [Belle Collaboration], Phys. Rev. Lett. **100**, 112001 (2008) [arXiv:0710.2577 [hep-ex]].
- [11] I. Adachi *et al.* [Belle Collaboration], arXiv:0808.2445 [hep-ex].
- [12] L. Maiani, A. D. Polosa and V. Riquer, Phys. Rev. D **98**, 054023 (2018) [arXiv:1803.06883 [hep-ph]].
- [13] A. Ali and W. Wang, Phys. Rev. Lett. **106**, 192001 (2011) [arXiv:1103.4587 [hep-ph]].
- [14] A. Ali, C. Hambroek and W. Wang, Phys. Rev. D **88**, 054026 (2013) [arXiv:1306.4470 [hep-ph]].
- [15] A. Bondar *et al.* [Belle Collaboration], Phys. Rev. Lett. **108**, 122001 (2012) [arXiv:1110.2251 [hep-ex]].
- [16] M. Tanabashi *et al.* [Particle Data Group], Phys. Rev. D **98**, 030001 (2018).
- [17] A. M. Badalian, B. L. G. Bakker and I. V. Danilkin, Phys. Atom. Nucl. **73**, 138 (2010) [arXiv:0903.3643 [hep-ph]].
- [18] S. Weinberg, Phys. Rev. Lett. **110**, 261601 (2013) [arXiv:1303.0342 [hep-ph]].
- [19] M. Knecht and S. Peris, Phys. Rev. D **88**, 036016 (2013) [arXiv:1307.1273 [hep-ph]].
- [20] R. F. Lebed, Phys. Rev. D **88**, 057901 (2013) [arXiv:1308.2657 [hep-ph]].
- [21] T. D. Cohen and R. F. Lebed, Phys. Rev. D **90**, 016001 (2014) [arXiv:1403.8090 [hep-ph]].
- [22] L. Maiani, A. D. Polosa and V. Riquer, JHEP **1606**, 160 (2016) [arXiv:1605.04839 [hep-ph]].
- [23] W. Lucha, D. Melikhov and H. Sazdjian, Phys. Rev. D **96**, 014022 (2017) [arXiv:1706.06003 [hep-ph]].
- [24] W. Lucha, D. Melikhov and H. Sazdjian, Eur. Phys. J. C **77**, no. 12, 866 (2017) [arXiv:1710.08316 [hep-ph]].
- [25] A. Ali, L. Maiani, and A. D. Polosa, *Multiquark Hadrons*. Cambridge University Press, Cambridge, 2019.
- [26] E. Witten, Nucl. Phys. B **160**, 57 (1979).
- [27] G. C. Rossi and G. Veneziano, Nucl. Phys. B **123**, 507 (1977).
- [28] L. Montanet, G. C. Rossi and G. Veneziano, Phys. Rept. **63**, 149 (1980).
- [29] T. Cohen, F. J. Llanes-Estrada, J. R. Pelaez and J. Ruiz de Elvira, Phys. Rev. D **90**, 036003 (2014) [arXiv:1405.4831 [hep-ph]].
- [30] G. Rossi and G. Veneziano, JHEP **1606**, 041 (2016) [arXiv:1603.05830 [hep-th]] and references therein.
- [31] L. Maiani, V. Riquer and W. Wang, Eur. Phys. J. C **78**, no. 12, 1011 (2018) [arXiv:1810.07848 [hep-ph]].
- [32] G. T. Bodwin, E. Braaten and G. P. Lepage, Phys. Rev. D **51**, 1125 (1995) Erratum: [Phys. Rev. D **55**, 5853 (1997)] [hep-ph/9407339].
- [33] P. M. Nadolsky *et al.*, Phys. Rev. D **78**, 013004 (2008) [arXiv:0802.0007 [hep-ph]].
- [34] A. D. Martin, W. J. Stirling, R. S. Thorne and G. Watt, Eur. Phys. J. C **63**, 189 (2009) [arXiv:0901.0002 [hep-ph]].
- [35] H. L. Lai *et al.*, Phys. Rev. D **82**, 074024 (2010) [arXiv:1007.2241 [hep-ph]].
- [36] L. S. Brown and R. N. Cahn, Phys. Rev. Lett. **35**, 1 (1975).